CANADIAN JOURNAL OF REMOTE SENSING
2018, VOL. 44, NO. 2, 131–143
https://doi.org/10.1080/07038992.2018.1461557

Taylor & Francis
Taylor & Francis Group

Check for updates

Transferability of Lidar-derived Basal Area and Stem Density Models within a Northern Idaho Ecoregion

Patrick A. Fekety[a*], Michael J. Falkowski[b], Andrew T. Hudak[c], Theresa B. Jain[c], and Jeffrey S. Evans[d,e]

[a]Department of Forest Resources, University of Minnesota, St. Paul, MN, USA; [b]Department of Ecosystem Science and Sustainability, Colorado State University, Fort Collins, CO, USA; [c]United States Forest Service, Rocky Mountain Research Station, Moscow, ID, USA; [d]The Nature Conservancy, Central Science, Fort Collins, CO, USA; [e]Department of Zoology and Physiology, University of Wyoming, Laramie, WY, USA

ABSTRACT

A patchwork of disjunct lidar collections is rapidly developing across the USA, often acquired with different acquisition goals and parameters and without field data for forest inventory. Airborne lidar and coincident field data have been used to estimate forest attributes across individual lidar extents, where forest measurements are collected using project-specific inventory designs. This research explores predicting forest attributes at locations not represented in the training data by combining lidar and field measurements from ecologically similar forests. Using field measurements from six lidar units, random forests regression models were created by systematically withholding forest inventory data from one lidar unit and using the forest inventory data from the other five units to predict basal area and stem density at the withheld unit. Results indicate that BA models produce more accurate predictions than stem density models when transferred to a lidar unit that did not contain field data. Relative root mean square errors calculated from the withheld field plots ranged between 32.3%–50.1% for BA and 40.7%–67.3% for stem density models. It is concluded that forest managers may use predictive models constructed from ecologically similar forests to obtain a preliminary estimate of resources, until local field measurement can be obtained.

RÉSUMÉ

Un ensemble disparate de collections de données lidar se développe rapidement aux États-Unis, souvent acquises avec des objectifs et des paramètres différents et sans données de terrains relatives aux inventaires forestiers. Des données de terrain concomitantes sont utilisées pour estimer des attributs forestiers au sein d'étendues de lidar aéroporté individuelles, pour lesquelles les mesures d'intérêt correspondent à des modèles d'inventaires déterminés. En combinant des mesures de terrain et de lidar provenant de forêts écologiquement similaires, cette étude examine la prédiction d'attributs forestiers à des endroits où des données d'entrainement sont absentes. En utilisant des mesures de terrain, des modèles de régression produits par des forêts d'arbres décisionnels ont été créés pour six unités de lidar. Un procédé systématique a été suivi par lequel les données de chaque unité sont retenues et la surface terrière et densité des tiges de cette unité sont ensuite estimés avec les données des cinq unités restantes. Les résultats indiquent que les estimations de surface terrière sont plus robustes que pour la densité de tiges lorsque les modèles sont transférés à une unité de lidar pour laquelle les données de terrain sont absents. Les erreurs quadratiques moyennes relatives calculées pour les échantillons retenus sont entre 32.3 % et 50.1 % pour les modèles de surface terrière et entre 40.7 % et 67.3 % pour la densité des tiges. Nous concluons que, jusqu'à ce que des mesures de terrain locales puissent être acquises, il est possible d'obtenir des estimations préliminaires de ressources forestières en utilisant des modèles prédictifs construits à partir d'échantillons de forêts écologiquement similaires.

ARTICLE HISTORY
Received 10 November 2017
Accepted 13 March 2018

Introduction

Airborne light detection and ranging (lidar) is widely used in forest management to meet various objectives (Maltamo et al. 2014) such as predicting timber volume (White et al. 2014), identifying forest structure characteristics important for wildlife habitat (Martinuzzi et al.

CONTACT Patrick A. Fekety patrick.fekety@colostate.edu
*Current Address: Colorado State University, Department of Ecosystem Science and Sustainability, Fort Collins, CO, 80523, USA

The work of Andrew Hudak and Theresa Jain was authored as part of their official duties as Employees of the United States Government and is therefore a work of the United States Government. In accordance with 17 USC. 105, no copyright protection is available for such works under US Law.

Patrick Fekety, Michael Falkowski and Jeffrey Evans hereby waive their right to assert copyright, but not their right to be named as co-authors in the article.

2009), and using high resolution lidar-derived digital terrain models (DTM) to locate forest roads (Aruga et al. 2005). As more lidar data are being acquired, a patchwork of disjunct datasets is developing across regional extents. In the United States, contiguous county and state-level lidar collections exist, although the motivation for large-scale collections is typically the development of high-resolution digital terrain models (DTMs), rather than characterizing forest vegetation (e.g., 3DEP 2016; MNGeo 2015). Field measurements describing vegetation are not typically collected when the lidar are acquired for non-forestry related objectives. However, forest managers typically establish inventory plots to provide training data for predictive models when lidar collections are motivated by forest management needs. To provide the most benefit, coincident plot-level field data are collected as temporally close to the lidar acquisition as possible (White et al. 2013; Eskelson et al. 2009). Although forest type and stand age will affect the ability to use non-temporally coincident data, field plots measured up to 5 years before the lidar collection have been used (Zald et al. 2014). Leveraging temporally appropriate inventory measurements and lidar data in ecologically similar areas may facilitate the prediction of forest inventory attributes to lidar collections that contain little or no local forest inventory measurements, thus transferring an existing predictive model to a new spatial location.

Managers need up-to-date information characterizing forest resources, such as basal area and stem density, to support both operational and long-term planning. Predictive modeling using lidar can provide resource estimates across large spatial extents (Næsset 2004) while repeat lidar collections allow the characterization of resource change (Hudak et al. 2012). Lidar data, in conjunction with coincident field data, have been used in predictive modeling of forest inventory attributes with success (e.g., Næsset 2002; R^2 0.80–0.93 for volume). Several studies have predicted forest attributes solely from disjunct lidar collections (Lefsky et al. 2002; Hudak et al. 2006; Næsset 2007). For example, Næsset (2007) constructed linear regression models to predict six forest inventory metrics by combining two lidar acquisitions, with similar collection parameters, that were 50 km apart in Norway and achieved excellent results (e.g., R^2 for volume ranged between 84% and 89%). Across a larger spatial extent, Lefsky et al. (2002) built a regression model to predict aboveground biomass across three North American biomes and achieved an R^2 of 0.84. Using full waveform lidar data and aerial imagery, Latifi and Koch (2012) created imputation models to predict forest attributes using various combinations of local and non-local data. They found that models built exclusively from non-local data resulted in the largest relative errors, but adding a portion of the withheld data substantially decreased the error. While the previous studies discussed spatially transferring models, Fekety et al. (2015) demonstrated the feasibility of temporally transferring lidar-based basal area imputation models and achieved satisfactory results (e.g., $R^2 = 0.78–0.79$). Combining spatially and temporally disjunct lidar data in a statistical modeling framework could allow for the creation of prediction models to estimate forest inventory data to newly acquired lidar collections, ultimately providing a first pass estimate of forest resources.

The overarching goal of this research is to create predictive models by combining spatially and temporally disjunct lidar and field data and evaluating performance when the model is transferred to locations where lidar data exist, but do not have ground truth measurements. We hypothesized transferring models to unsampled, yet ecologically similar, forests will produce predictions that are statistically equivalent to ground truthed values. To achieve this goal, we leverage a database consisting of six independently collected field datasets and six spatially and temporally disjunct lidar collections throughout northern Idaho. A series of models were created by systematically withholding field data from one lidar unit and treating the withheld data as a validation dataset. This procedure may provide resource managers with acceptable estimates of forest attributes at locations that do not have local field data.

Methods and materials

Study area

The study area for this project is the Inland Northwest region of the Northern Rocky Mountain ecoregion (Figure 1). Forests in the Inland Northwest are mixed conifer with Douglas-fir (*Pseudotsuga menziesii* (Mirb.) Franco), grand fir (*Abies grandis* (Douglas ex D. Don) Lindl.), western redcedar (*Thuja plicata* Donn ex D. Don), and western hemlock (*Tsuga heterophylla* (Raf.) Sarg.) as the primary climax species (Cooper et al. 1991). The region is occupied by primarily north–south mountain ranges separated by intermontane valleys (Taylor 2012). The study area encompasses elevations between 650 m and 2000 m (mean 1090 m) and slopes up to 65% (mean 33%). Geology is a mixture of the sedimentary Belt Supergroup and Idaho Batholith granitics (Cooper et al. 1991); local ash caps deposited by the Mount Mazama eruption (*c*.5700 BCE) created localized pockets of highly productive forests (Kimsey et al. 2008).

Climate is moderated by the maritime influences of the Pacific Ocean. Precipitation is greater at higher elevations, caused by orographic lifting, with the majority of precipitation occurring in the winter.

This study focuses on six locations distributed throughout northern Idaho that have associated field and lidar measurements. Priest River Experimental Forest (PREF) is a 2,758 ha forest managed by the U.S. Forest Service, Rocky Mountain Research Station, located approximately 18 km north of Priest River, ID and noted for its diverse mixed conifer forest. The 12,948 ha Fernan lidar extent covers the Fernan, Blue Creek, and Wolf Lodge watersheds, which drain into the north end of Lake Coeur d'Alene. Sixty-six percent of the Fernan extent is private land consisting of private industrial forest, agricultural, and wildland urban interface, while the remaining 34% is public forest primarily managed by the U.S. Forest Service as part of the Coeur d'Alene Ranger District of the Idaho Panhandle National Forests. The Tepee Potter lidar unit covers 11,737 ha and is also managed by the Idaho Panhandle National Forests and is 39 km east of Coeur d'Alene, ID. The Moscow Mountain 19,889 ha study area located 18 km from Moscow, ID is primarily private industrial forests (43%) with inholdings of private non-industrial forests (39%) and state lands (18%). The St. Joe project area (Figure 1) is 55,723 ha managed mainly by private timber companies (62%) and the Idaho Panhandle National Forests (38%). The 10,864 ha area referred to as Upper Lolo is managed by the Nez Perce-Clearwater National Forests and is located 38 km northwest of Kooskia, ID.

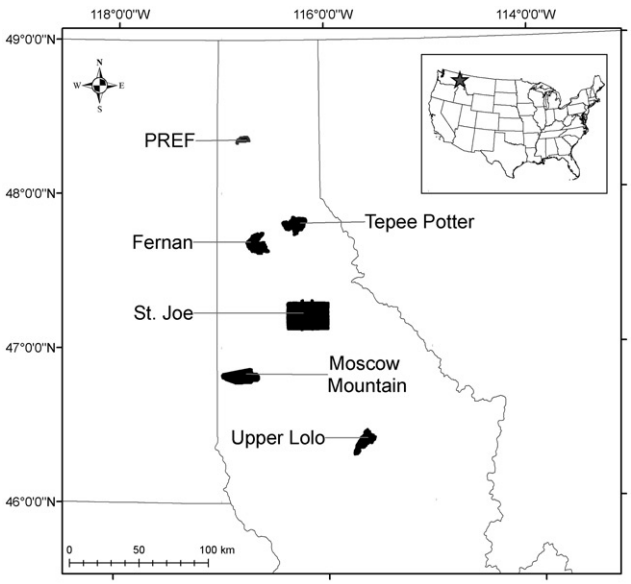

Figure 1. Location of project areas within Inland Northwest.

Field plot data

Six independent field data collection exercises were performed within the six lidar extents and sampling concluded within a year of the respective lidar collection. The field data were collected for various reasons and therefore differ in sampling design and data collection protocols. At a minimum, all study designs called for a complete inventory of live and standing dead trees with a diameter breast height (DBH) greater than 12.7 cm to be measured within the plots. Measurement protocols for smaller trees varied among inventory designs and were excluded from these analyses. All field plots were geolocated with a Trimble (Sunnyvale, CA, USA) global navigation satellite system (GNSS) and differentially corrected using local base stations. In total, 360 field plots throughout the Inland Northwest were used in this study (Table 1). Field plot locations were located following stratified random designs, which were specific to each data collection exercise. The landscape stratification for field plots located on the Coeur d'Alene River District (herein referred to as CdA) data require further explanation because the stratified random design considered both the Fernan and Tepee Potter lidar units. Consequently, for this study, the field measurements were separated into two datasets based on their coincident lidar unit; CdA-East plots ($n = 24$) were located in the Tepee Potter lidar unit while the CdA-West plots ($n = 10$) were located in the Fernan lidar unit. The CdA-East plots were combined with the Tepee Potter plots for model construction.

Table 1. Field data collection parameters.

Field dataset	*n*	Year	Lidar unit	Plot Area (m^2)	Plot design	Sampling design
CdA-East	24	2015	Tepee Potter	400	Fixed radius	Stratified by elevation, transformed aspect, and wetness
CdA-West	10	2015	Fernan	400	Fixed radius	Stratified by elevation, transformed aspect, and wetness
Moscow Mtn.	85	2009	Moscow Mtn.	400	Fixed radius	Stratified by elevation, solar insolation, and NDVIc
PREF	96	2011	PREF	400	Fixed radius	Stratified by forest type and canopy cover
St. Joe	79	2003-2004	St. Joe	400	Fixed radius	Stratified by elevation and solar insolation
Tepee Potter	39	2014	Tepee Potter	400	Fixed radius	Stratified by elevation, solar insolation, and NDVI
Upper Lolo	27	2007	Upper Lolo Creek	400	Fixed radius	Stratified by elevation, transformed aspect, and NDVIc

Note: CDA-East and CDA-West were part of the same data collection exercise. Both Tepee Potter and Fernan lidar units were combined for the stratification.
NDVI: Normalized difference vegetation index.
NDVIc: Normalized difference vegetation index corrected by middle infrared.

Table 2. Summary of plot-level basal area and stand density estimates.

			Basal area (m^2/ha)					Stem sensity (stems/ha)				
Project	Total plots	Treeless plots	Min	Mean	Median	Max	SD	Min	Mean	Median	Max	SD
CdA-East	24	3	0	34	32	88	21	0	403	436	872	252
CdA-West	10	1	0	20	19	49	15	0	229	212	598	195
Moscow Mountain	85	6	0	25	21	109	21	0	358	299	1122	285
PREF	96	9	0	31	27	99	24	0	387	349	1645	320
St. Joe	79	1	0	37	37	112	24	0	543	449	1570	348
Tepee Potter	39	1	0	30	32	93	18	0	403	449	872	229
Upper Lolo	27	6	0	35	36	92	26	0	300	324	623	208
All projects	360	27	0	31	29	112	23	0	406	374	1645	304

Note: CdA-East and CdA-West were collected during a single campaign. Both Fernan and Tepee Potter lidar collections were combined for this stratification.

Table 3. Lidar collection parameters.

Lidar Collection	Fernan	Moscow Mountain	PREF	St. Joe	Tepee Potter	Upper Lolo
Date collected	Dec 2014 & Feb 2015	Jun 2009	July 2011	Summer 2003	May 2015	Sept–Oct 2006
Vendor	QSI Environmental	Watershed Sciences, Inc	Watershed Sciences, Inc	Horizons, Inc.	QSI Environmental	Watershed Sciences, Inc.
Sensor	Leica ALS 70 and ALS 80	Leica ALS50 Phase II	Leica ALS50 Phase II	Leica ALS40	Leica ALS 70	Leica ALS50 Phase II
Pulse frequency	195 kHz[a]	N/A	73.5 kHz	20 kHz	180 kHz[a]	83 kHz
Scan angle	+/– 15 degrees	+/– 14 degrees	+/– 15 degrees	+/– 15 degrees	+/– 15 degrees	+/– 14 degrees
Altitude	1,400 m AGL	2,000 m AGL	1,500 m AGL	2,438 m AGL	1,450 m AGL	1,100 m AGL
Spatial extent	12,948 ha	19,889 ha	4,041 ha	55,723 ha	11,737 ha	10,864 ha
Wavelength	1,064 nm	1,064 nm	1,064 nm	1,064 nm	1,064 nm	1,064 nm
Vertical accuracy	3.4 cm	4.3 cm	4.9 cm	N/A	5.8 cm	6.3 cm
Pulse density	16.4 pulses/m^2	8.5 pulses/m^2	10.4 pulses/m^2	0.6 pulses/m^2	20.8 pulses/m^2	4.7 pulses/m^2
Footprint	31 cm	30–45 cm	34 cm	30 cm	32 cm	24 cm

Note: AGL: above ground level.
N/A: not available.
[a]Operating "Single Pulse in Air" mode.

Response variables

The response variables predicted were BA and stem density, which are valuable for regional scale forest management and planning. Summary statistics for the response variables are found in Table 2.

Explanatory variables

Data from six independent, discrete-return, airborne lidar collections located within the Inland Northwest of northern Idaho, USA were used for this study (Figure 1). Lidar were collected with Leica lidar scanners; however, differences in acquisition parameters varied considerably between some of the acquisitions, largely resulting from lidar sensor improvements across the 12-year time period considered in this study (Table 3). All of the lidar datasets were collected in snow-free conditions, which can limit the window of lidar collections, especially at higher elevations within the study area. With the exception of western larch (*Larix occidentalis*), the major tree species in the study area are evergreen, and consequently in a persistent leaf-on state. The Fernan lidar data were collected while deciduous understory shrubs were in leaf-off conditions.

When available, the vendor-identified ground returns were accepted as accurately classified. Fernan and Tepee Potter ground returns were identified by the vendor using TerraScan V.15 (Terrasolid Ltd, Helsinki, Finland). Ground returns within the PREF lidar extent were classified with Lidar Feature Extraction – the vendor's proprietary classification algorithm. The lidar vendor did not classify ground returns for the Moscow Mountain, St. Joe and Upper Lolo lidar collections; therefore, ground returns were identified using the multi-scale curvature classification (MCC)-lidar algorithm (Evans and Hudak 2007), which fits a multi-scale thin plate spline model to classify lidar ground returns. A 1-m DTM was generated from the classified ground returns using FUSION v3.60 (McGaughey 2016) for the Fernan, Moscow Mountain, PREF, Tepee Potter, and Upper Lolo lidar collections. The lidar pulse density at St. Joe was insufficient to generate a 1-m DTM (Table 3); therefore, a 2-m DTM was generated. Figure 2 shows a conceptual model describing the lidar processing and model building processes.

Lidar returns that fell within the field plots were extracted using FUSION (McGaughey 2016) and height-normalized point clouds were generated via DTM subtraction. Following the results of Næsset

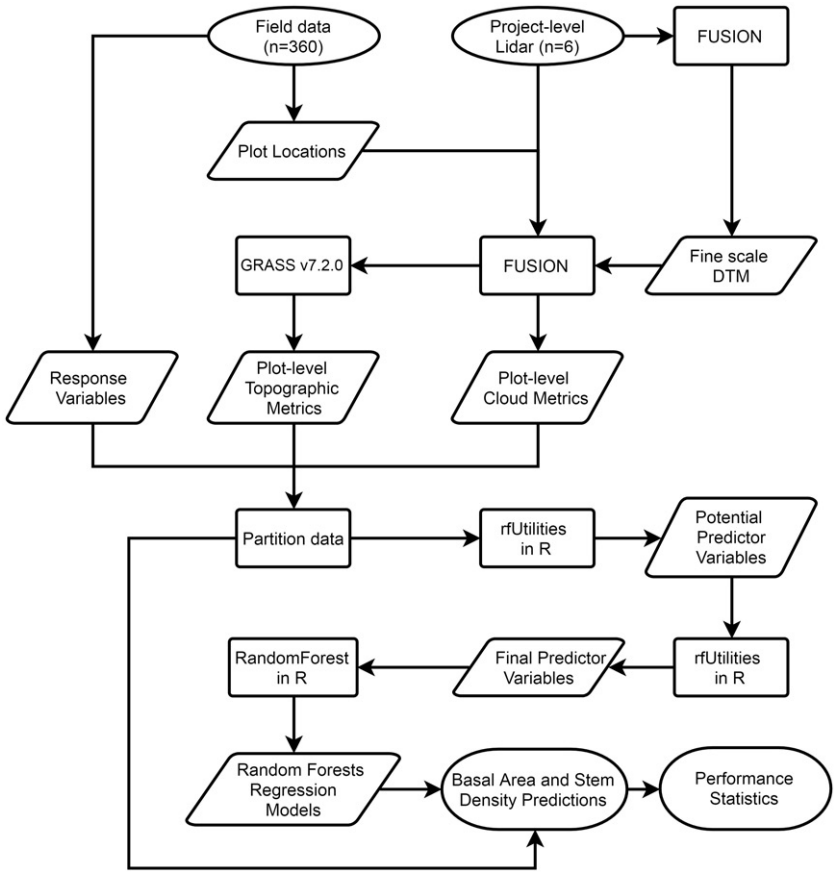

Figure 2. Conceptual model describing major steps of the lidar processing and model building.

(2009) and Bater et al. (2011), plot-level point clouds consisting of only first returns were processed with FUSION to calculate plot-level height, strata, and cover metrics. A 1.37 m (equivalent to breast height) cutoff was used when calculating lidar height and cover metrics.

Topographic metrics influence forest productivity (Stage and Salas 2007), and thus stand conditions. FUSION was used to create gridded rasters of elevation, slope, and aspect, which were inputted to Geographic Resources Analysis Support System v7.2.0 (GRASS Development Team 2017) to create additional topographic metrics. A full list of predictor variables can be found in Table 4.

Model specification: random forests regression

Random forests (Breiman 2001) regression models were created using the randomForest package (Liaw and Wiener 2002) in R statistical software (R Core Team 2017) to predict BA and stem density. Numerous papers describe the random forests algorithm applied in a natural resource context (e.g. Prasad et al. 2006; Lawrence et al. 2006; Cutler et al. 2007). Six BA and six stem-density prediction models

Table 4. Potential explanatory variables.

Description of explanatory variables	Data source
H05Pct: Height 5th percentile	FUSION
H25Pct: Height 25th percentile	FUSION
H50Pct: Height 50th percentile	FUSION
H75Pct: Height 75th percentile	FUSION
H95Pct: Height 95th percentile	FUSION
Hmean: Height mean	FUSION
Hstdv: Height standard deviation	FUSION
Hskew: Height skewness	FUSION
Hkurt: Height kurtosis	FUSION
CRR: Canopy relief ratio (McGaughey 2016)	FUSION
Stratum 0: Percentage lidar returns <0.15 m	FUSION
Stratum 1: Percentage lidar returns >0.15 m and <1.37 m	FUSION
Stratum 2: Percentage lidar returns >1.37 m and <5.0 m	FUSION
Stratum 3: Percentage lidar returns >5 m and <10 m	FUSION
Stratum 4: Percentage lidar returns >10 m and <20 m	FUSION
Stratum 5: Percentage lidar of returns >20 m and ≤0 m	FUSION
Stratum 6: Percentage lidar of returns >30 m	FUSION
Pct1Rtn_1.37: Percentage lidar first returns above 1.37 m	FUSION
Pct1Rtn_mean: Percentage lidar first returns above height mean	FUSION
Elev: DTM elevation at 20 m resolution	FUSION
Slope: Percent slope at 20 m resolution	FUSION
TrAsp: Transformed aspect at 20 m resolution	Calculated in R
SCOSA: Slope cosine aspect transformation	Calculated in R
SSINA: Slope sine aspect transformation	Calculated in R
GlobRadEquinox: Radiance estimate on 23 Sept	GRASS
accumulation: Hydrologic flow accumulation	GRASS
tci: Topographic convergence index	GRASS
twi: Topographic wetness index	GRASS

were created by systematically withholding the reference observations that were located in one of the six lidar units. The resulting models are used to evaluate how well a given model could be expected to perform when transferred to a new lidar unit (represented by the withheld area). In this study the models are designated by the name of the lidar unit to which they will be transferred. For example, the Fernan models are used to predict BA and stem density at sites located in the Fernan lidar unit and trained using field and lidar data collected in the Moscow Mountain, PREF, St. Joe, Tepee Potter, and Upper Lolo lidar units.

Model selection process

We expected many of the potential explanatory variables to be highly correlated (Spearman rank correlation coefficient >0.85), and it was anticipated that some lidar metrics would also exhibit multi-collinearity; therefore, the rfUtilities R library was used to perform a Gram-Schmidt QR-decomposition to identify and remove multi-collinear variables (Evans and Murphy 2017; Falkowski et al. 2009). Multi-collinear variables were identified and removed before constructing each model.

A model selection tool centered on the random forests algorithm (Breiman 2001) was used in the model selection processes. Model selection was performed using the rf.modSel function from the rfUtilities package to select the best suite of predictor variables for each response variable (Murphy et al. 2010). Through an iterative process, the function builds a random forests model consisting of all potential predictor variables and subsequently builds additional models by eliminating the potential predictor variable with the lowest model improvement ratio (MIR). The process is repeated until the model error does not change or a single variable remains. The selected parameters are associated with the model exhibiting the greatest percentage variation explained and the least squared-error. The results from the rfUtilities model selection process were used to specify the models. In all cases, the model selection tool was run 100 times for each response variable to investigate the stability in the selected model.

Model evaluation

The predictive models were evaluated with both internal fit statistics and performance statistics. The random forests models fit statistics were calculated with the rf.crossValidation function from rfUtilities (Evans and Murphy 2017). Cross-validated estimates of root-mean-square error (RMSE; Equation 1) were calculated between the observed and predicted values using the training data. RMSE was normalized by the mean observation to allow for comparisons among the models (Equation 2).

$$\mathrm{RMSE} = \sqrt{\frac{1}{n}\sum(predictions - observations)^2} \quad [1]$$

$$\mathrm{RMSE\%} = \frac{\mathrm{RMSE}}{mean(observations)} * 100\% \quad [2]$$

where RMSE% is the normalized RMSE. The median percentage variation explained (pseudo-R^2) and RMSE% were reported, along with their standard deviations, for 100 cross-validations.

RMSE% was also reported as a performance statistic and was calculated using the withheld data and its complementary predictions in order to determine how well a model would transfer to a new area.

Predictions were further evaluated using statistical equivalence tests. Standard t-tests were not used because they are designed to test for differences, not similarities, between two statistics (Robinson and Froese 2004). Failure to reject the null hypothesis for a standard t-test suggests there is not sufficient evidence that two datasets are not equal; however, this does not guarantee that two datasets are similar because the statistical power of the chosen test might be weak (Robinson and Froese 2004). Statistical equivalence tests set the null hypothesis such that the datasets are dissimilar and requires the data to prove otherwise. Generic forms for the hypotheses are:

H0: Model predictions are dissimilar to observed values; and

H1: Model predictions are similar (i.e. equivalent) to observed values.

Equivalence tests were performed in R using the bootstrapped implementation from the equivalence package (i.e. equiv.boot; Robinson 2016), which uses the two one-sided test (TOST) of equivalence. The TOST examines if the intercept ($\beta 0$) and slope ($\beta 1$) estimators from the linear regression between the model predictions and true values are contained in a predetermined region of equivalence. The intercept component of the equivalence test is a measure of bias, whereas the slope component is a measure of proportionality (Robinson et al. 2005). In this study, the test of bias determines if the mean of the observations is equivalent to the mean of the predictions; the test for proportionality determines if the slope between model predictions and observations is equivalent to one.

Table 5. Explanatory variables used in basal area and stem density random forests models.[a]

	Basal Area						Stem Density					
Explanatory Variable	Fernan	Moscow Mtn.	PREF	St. Joe	Tepee Potter	Upper Lolo	Fernan	Moscow Mtn.	PREF	St. Joe	Tepee Potter	Upper Lolo
H05Pct	X		X	X	X	X	X	X	X	X	X	X
H95Pct	X		X	X	X	X						
Hmean		X										
Pct1Rtn_mean	X	X	X	X	X	X	X	X	X	X	X	X
Stratum 0								X			X	
Stratum 1	X			X	X		X	X	X	X	X	X
Stratum 2			X									
Stratum 3										X		
Stratum 4	X	X	X	X	X		X	X	X	X	X	X
Stratum 5	X	X	X	X	X	X	X	X	X		X	X
Stratum 6		X										

Note: X: selected variable. [a]See Table 4 for description of explanatory variables.

Table 6. Median cross-validated model fit statistics (and standard deviation) for basal area and stem-density models.

Response	Model	Variance Explained (%)	SD (%)	RMSE% (%)	SD (%)
Basal area	Fernan	76.9	(1.0)	35.2	(5.6)
	Moscow Mountain	73.3	(1.1)	34.9	(6.8)
	PREF	76.7	(0.9)	32.0	(6.7)
	St. Joe	76.8	(1.2)	35.2	(6.9)
	Tepee Potter	76.7	(1.0)	36.9	(6.4)
	Upper Lolo	79.1	(0.8)	32.5	(5.0)
Stem density	Fernan	65.6	(1.3)	42.5	(5.5)
	Moscow Mountain	64.4	(1.4)	43.7	(7.1)
	PREF	61.8	(1.5)	44.7	(6.9)
	St. Joe	65.5	(1.0)	43.8	(8.4)
	Tepee Potter	69.1	(1.1)	42.4	(7.7)
	Upper Lolo	65.6	(1.3)	43.9	(6.6)

If the confidence intervals (CI) from the TOST around the estimator (i.e., intercept or slope) are entirely contained within the region of equivalence then there is evidence to reject the null hypothesis, meaning the two data sets are statistically equivalent. The default region of equivalence of ±25% was used in this study and has been called a conservative region of equivalence (Wellek 2003; Robinson and Froese 2004) and has been used in other studies (e.g., Falkowski et al. 2008; Penner et al. 2013). Additionally, the exact regions of equivalence were calculated to determine the smallest region of equivalence when the null hypothesis is no longer rejected. A smaller region of equivalence indicates better agreement between the observations and predictions. The region of equivalence for bias was calculated as a percentage and in absolute units (i.e., m^2/ha or stems/ha). The region of equivalence for proportionality was calculated only as a percentage because the slope is dimensionless.

Results

Nineteen lidar height metrics and 9 topographic metrics were considered as potential explanatory variables (Table 4). After removing multi-collinear variables and performing the model selection process, the explanatory variables were pared down to a subset of only lidar height metrics (Table 5).

BA and stem density random forests prediction models were created and subsequently used to predict BA and stem density at the field plots that were withheld from the model training. Cross-validation fit statistics calculated solely from the training data showed better fit for the BA models than the stem density models in terms of variance explained and RMSE% (Table 6). When comparing the predictions with withheld observations, RMSE% performance statistics were within one standard deviation of the cross-validated RMSE% fit statistics for 10 out 12 models – Upper Lolo BA model and Fernan stand density model performance RMSE% were greater than one standard deviation (Tables 6 and 7).

Equivalence tests show BA predictions for Moscow Mountain, PREF, and Tepee Potter were statistically equivalent to the measured BA, in terms of both bias and proportionality at a ± 25% region of equivalence (Figure 3A). The 95% CI of the bias component for the Fernan BA predictions extends outside the lower region of equivalence indicating positive biases (i.e., over-predictions). These over-predictions can also be seen by investigating the scatter plot in Figure 4A, which shows 9 of the 10 Fernan BA predictions were larger than the observed value. When the 95% CI of the bias component extends outside the upper region of equivalence, such as with the Upper Lolo BA predictions, this indicates that the model is under-predicting the attribute on average (Figure 3A). The 95% CI of proportionality component extends outside the lower range of region of equivalence for Fernan and Upper Lolo BA predictions, which denotes that model over-predicts low BA plots and under-predicts high BA plots. Likewise, the 95% CI of proportionality component extends outside the upper range of region of equivalence for St. Joe denoting that model

Table 7. Model performance reported as normalized root-mean-square error (RMSE%) and the region of equivalence limit when the equivalence test no longer rejects the null hypothesis.

		Basal Area				Stem Density			
Model	*n*	RMSE% (%)	R0 (m^2/ha)	R0 (%)	R1 (%)	RMSE% (%)	R0 (stems/ha)	R0 (%)	R1 (%)
Fernan	10	33.8	±8.5	±26.5	±29.7	67.3	±184.2	±53.1	±52.2
Moscow Mountain	85	35.9	±2.5	±7.9	±12.5	40.7	±36.0	±10.4	±21.1
PREF	96	40.0	±5.5	±17.1	±17.9	47.6	±86.2	±24.8	±17.3
St. Joe	79	33.4	±6.8	±21.3	±32.6	43.0	±127.0	±36.6	±20.0
Tepee Potter	63	32.3	±2.7	±8.6	±20.2	44.4	±51.5	±14.8	±39.7
Upper Lolo	27	50.1	±10.3	±32.2	±47.5	48.3	±100.7	±29.0	±48.2

Note: R0: region of equivalence for bias.
R1: region of equivalence for proportionality.

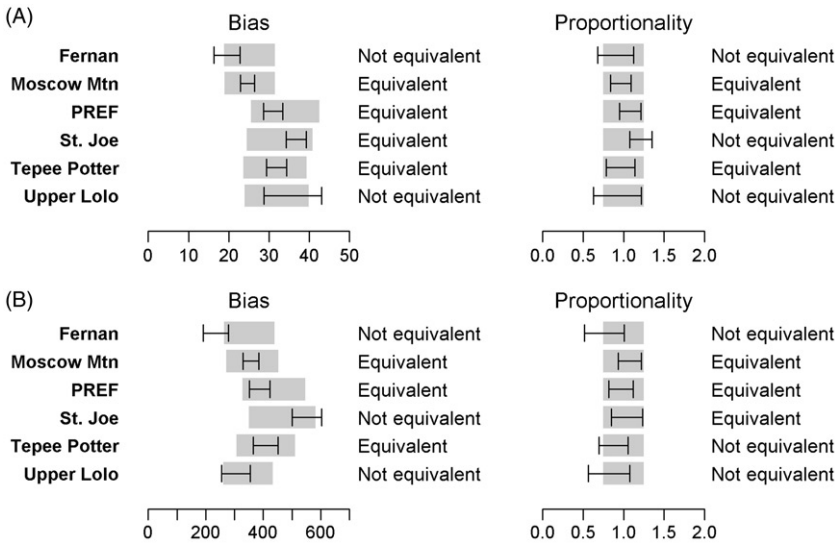

Figure 3. Results of bootstrapped equivalence tests for (A) basal area, and (B) stem density. The tests of biases are centered on the mean observation and the test of proportionality is centered on a slope of one. The shaded polygon represents the region of equivalence. The black bars represent the 95% confidence interval (CI). The equivalence test is satisfied when the 95% CI is completely contained in the region of equivalence.

under-predicts low BA plots and over-predicts high BA plots. In addition to the predetermined ±25% region of equivalence, the limit at which the equivalence test fails was also calculated (Table 7). Graphically, these values indicate the point when the 95% CI and region of equivalence share an edge. As previously stated, the Fernan predictions were not equivalent at a ± 25% region of equivalence; Table 7 shows the minimum acceptable region of equivalence as ±26.5% and ±29.7% for slope and proportionality, respectively. The bias region of equivalence can be converted to absolute units; for example the ±26.5% region of equivalence for the Fernan BA indicates the predictions are statistically equivalent to the observations if biases of up to ±8.5 m^2/ha of basal area are acceptable.

The stem-density models have larger errors compared with the BA models (see Table 7) and is also seen by the wider dispersion around the 1-to-1 line in Figure 5. Equivalence tests show stem-density predictions for Moscow Mountain and PREF were equivalent, in terms of bias and proportionality, to the measured stem density (Figure 3B). Moscow Mountain stem density was the best performing model as indicated by the narrowest calculated regions of equivalence (see Table 7). Fernan, Tepee Potter, and Upper Lolo 95% CI around the proportionality component of the equivalence test extends past the lower region of equivalence. These models over-predict less dense stands and under-predict denser stands. The stem-density predictions for the Fernan model are considerably over-predicted as seen by the small proportion of overlap between the 95% CI and region of equivalence (Figure 3B) and this is also apparent by investigating the scatter plot in Figure 5A.

Discussion

We evaluated the effectiveness of transferring random forests models to predict forest attributes in areas where lidar exist, but forest inventory measurements do not. This was achieved by combining several

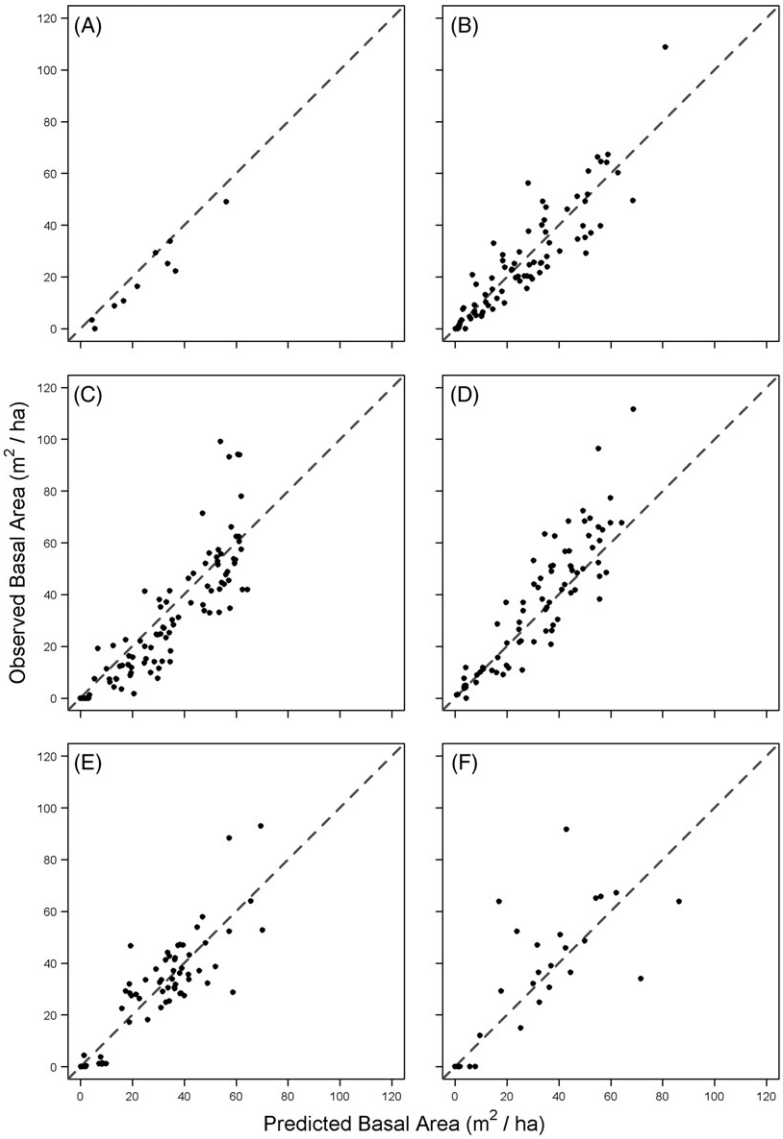

Figure 4. Observed versus independently predicted basal area estimates for: (A) Fernan; (B) Moscow Mountain; (C) PREF; (D) St. Joe; (E) Tepee Potter; (F) Upper Lolo. The dashed line is 1-to-1.

disjunct lidar and forest inventory datasets into models that predicted BA and stand density and transferring the model to lidar units excluded from the training data. Model performance was evaluated by calculating errors (RMSE%) and equivalence tests. We learned several lessons surrounding the combination of disjunct lidar acquisitions and field data for predicting forest inventory data to lidar collections without local reference observations. The remainder of the discussion covers these points in greater detail.

Model specification

Random forests modeling is one of many prediction methods used in natural resource applications and it was not our intention to test whether random forests provides the best results. Studies have shown that random forests outperformed (e.g. Coulston et al. 2012; Fassnacht et al. 2014), under-performed (e.g. Hayashi et al. 2015; Gleason and Im 2012), or performed similarly to (e.g. Freeman et al. 2014) other modeling techniques. Our intent was to build a parsimonious model which emulated the process that a resource manager could take to predict forest attribute at locations without field data; other modeling techniques could be explored.

Modelling considerations

The extent of a lidar collection is often defined by management boundaries (e.g., PREF) or watershed boundaries (e.g., Fernan, Tepee Potter, or Upper Lolo) and field data are not routinely collected when lidar are acquired for non-forestry applications. As more

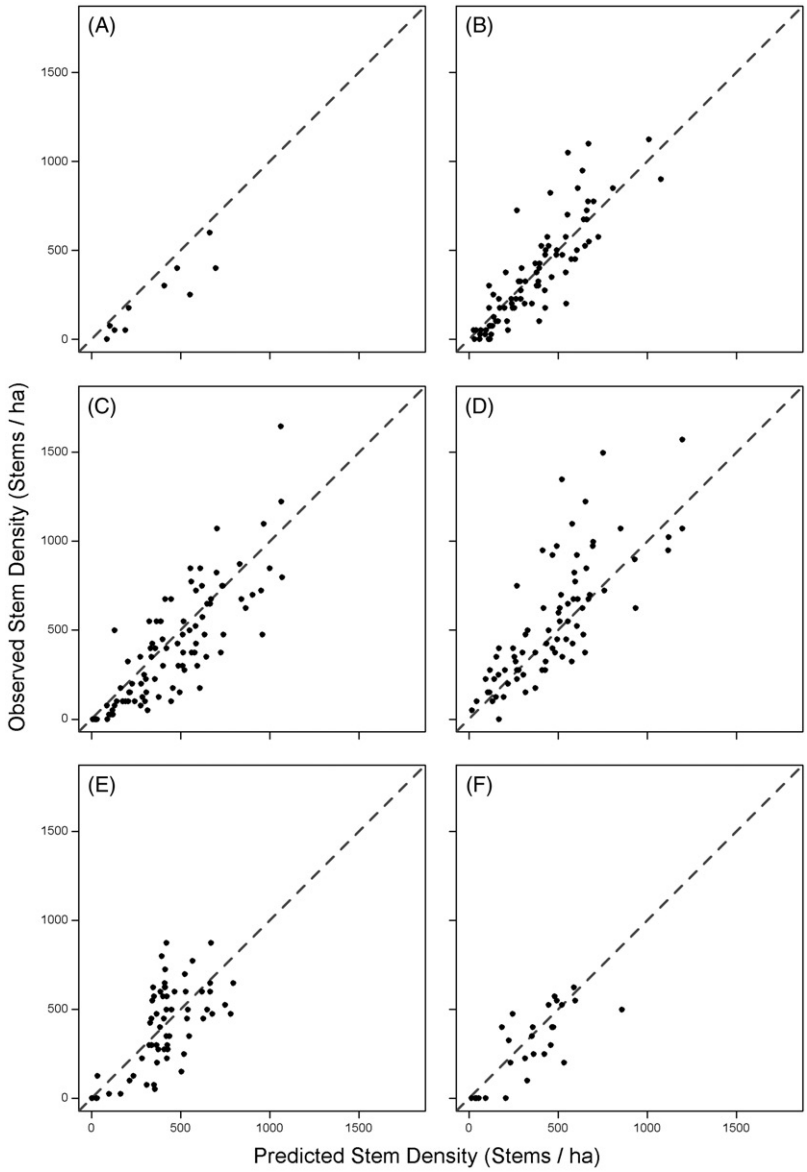

Figure 5. Observed versus independently predicted stand density estimates for: (A) Fernan; (B) Moscow Mountain; (C) PREF; (D) St. Joe; (E) Tepee Potter; (F) Upper Lolo. The dashed line is 1-to-1.

disjunct lidar are collected, regional models created from existing field data could be informative at providing larger-scale estimates of desired forestry attributes; for example, state or provincial-level estimates of forest resources. Transferring an existing forest attribute prediction model would also increase the utility of lidar collections that lack accompanying forest inventory data.

Managers and researchers creating prediction models may want to limit the reference observations to data collected with similar lidar collection parameters. Various lidar sensors and sensor settings can impact the resultant data and derived predictions when combining data from spatially or temporally disjunct acquisitions. Numerous studies have investigated the impacts that differences in lidar sensors, altitude, and pulse frequency have on data quality and accuracy (Goodwin et al. 2006; Hopkinson 2007; Næsset 2009). Variability in lidar processing parameters can also impact the metrics produced, and thus model results. Calculating metrics from 1st returns instead of all returns can produce more stable height metrics (Bater et al. 2011; Næsset 2009), which may be more appropriate when combining datasets. Collection parameters among disjunct lidar data inevitably vary, although many acquisitions achieve minimum standards (e.g., Heidemann 2014) to be acceptable for topographic use. These standards help ensure quality lidar data are collected and provide the opportunity for future use.

Extrapolations of any predictive model outside the extent covered by the reference observations must be used cautiously. Limiting the predictive model to an

ecologically similar extent should help ensure that the forest type, and thus lidar structural signatures, will be comparable. This study was limited to an ecologically similar study region, with similar tree species and forest structures (Bailey 1983). Ideally, field plots established using a single inventory design that spanned an entire ecoregion would be used to generalize predictions across spatially disjunct lidar collections. The unfortunate reality is that an inventory design is established to meet goals for a particular local project and not necessarily for use in a regional study. As disjunct datasets increase, it might be beneficial to post-stratify the field plots to obtain a sample that better represents the regions of interest. In this study, we assembled a database composed of field plots using different inventory designs yet demonstrated that this need not preclude their more generalizable utility. Researchers and managers planning field data collection for new lidar acquisitions should consider how new data can be optimally collected and incorporated into existing datasets.

Need for a standardized sampling protocol

The field data used in this study were not collected to investigate transferring models to areas without field data; instead they were collected for project-specific purposes. Different sampling protocols inevitably were a source of variation that could not be quantified in this study. There were common parameters in the sampling protocols including plot size, shape, and the fact plots followed stratified random sampling designs; however, the stratifications were performed to meet project-specific goals, not the goal of this study. The strata used to assign sampling locations can be grouped into topographic (e.g.; elevation), spectral (e.g.; NDVI), or biological (e.g.; forest type) categories (see Table 1). While sampling designs based on lidar metrics would better ensure that all the forest structures are captured, such implementation would require the lidar to be collected, processed, and delivered before any sampling could take place, which is often impractical due to budget cycles.

The lidar units in this study administratively fall within United States Forest Service (USFS) Region 1. Although the study area was a mixture of public and private land, the field data were collected by public agencies. Region 1, along with other USFS regions, has developed protocols for measuring field data in lidar units (USFS 2016); however, protocols across regions are not consistent. Managers and researchers are encouraged to consult existing protocols in lieu of creating their own and adapt existing protocols to meet not just their project-specific objectives but broader planning and management goals as well.

Conclusions

Random forests regression models were created to predict BA and stand density using 360 field plots and six lidar collections. The data were partitioned to investigate spatially transferring a model to a location that had lidar data but no field data. Topographic variables considered as predictors were not selected as being important but might exhibit greater importance at larger spatial scales. Although the field plots were collected using different sampling protocols, and the lidar were collected using different acquisition parameters, 3 out of 6 transferred models for BA were statistically equivalent in both bias and proportionality, whereas 2 out of 6 transferred models for stem density were statistically equivalent in both bias and proportionality. RMSE% performance statistics were within one standard deviation of the cross-validated RMSE% fit statistics for 5 out of 6 BA models and 5 out of 6 stem-density models, lending evidence that models can be transferred to lidar units that lack field data.

This work supports extending lidar-based prediction models to lidar extents that do not have tree data, assuming the structural characteristics of the unmeasured forest were included in the original predictive model but measured elsewhere within the ecoregion. The practice of spatially transferring models should not be a substitute for local forest inventory, but might provide reasonable estimates of forest attributes until managers are able to collect inventory data in unsampled lidar acquisition areas. Users of this technique must be willing to accept higher levels of error when predicting forest attributes to lidar collections that do not have field data. This study is limited to the Inland Northwest and more work is needed to determine if this procedure is applicable to other ecoregions, especially those with larger deciduous tree components.

Acknowledgments

This research was funded by the NASA New Investigator Program (Award #NNX14AC26G; Falkowski, Principal Investigator) and the NASA Carbon Monitoring Systems Program (Award #NNH15AZ06I; Hudak, Principal Investigator). Lidar and field data collections were paid for by the U.S. Forest Service via the Rocky Mountain Research Station (PREF, St. Joe), Nez Perce-Clearwater National Forest (Upper Lolo), Idaho Panhandle National Forests

(Tepee Potter), and Big Sky Partnership (Moscow Mountain). Fernan data were paid for through a partnership between Kootenai-Shoshone Soil and Water Conservation District (funding from Idaho Department of Lands) and the University of Idaho (funding from NSF EPSCoR via the Managing Idaho's Landscapes for Ecosystem Services (MILES) pilot study). Thanks are offered to Aaron Weiskittel for comments on an early version of this manuscript. Finally, the authors would like to thank the anonymous reviewer who provided comments that improved this manuscript.

References

3DEP (3D Elevation Program) 2016. U.S. Department of Interior, U.S. Geological Survey. http://nationalmap.gov/3DEP/index.html.

Aruga, K., Sessions J., and Akay, A.E. 2005. "Application of an airborne laser scanner to forest road design with accurate earthwork volumes." *Journal of Forest Research*, Vol. 10: pp.113–123. doi:10.1007/s10310-004-0116-9.

Bailey, R.G. 1983. "Delineation of ecosystem regions." *Environmental Management*, Vol. 7(No. 4): pp. 365–373. doi:10.1007/BF01866919.

Bater, C.W., Wulder, M.A., Coops, N.C., Nelson, R.F., Hilker, T., and Næsset, E. 2011. "Stability of sample-based scanning-LiDAR-Derived vegetation metrics for forest monitoring." *IEEE Transactions On Geoscience and Remote Sensing*, Vol. 49(No. 6): pp. 2385–2392. doi:10.1109/TGRS.2010.2099232.

Breiman, L. 2001. "Random forests." *Machine Learning*, Vol. 45(No. 1): pp. 5–32. doi:10.1023/A:1010933404324.

Cooper, S.V, Neiman, K.E., Roberts, D.W. 1991. "Forest habitat types of northern Idaho: A second approximation." United States Department of Agriculture. GTR INT-236. https://www.treesearch.fs.fed.us/pubs/24623

Coulston, J.W., Moisen, G.G., Wilson, B.T., Finco, M.V., Cohen, W.B., and Brewer, C.K. 2012. "Modeling percent tree canopy cover: a pilot study." *Remote Sensing*, Vol. 78(No. 7): pp. 715–727.

Cutler, D.R., Edwards, T.C. Jr., Beard, K.H., Cutler, A., Hess, K.T., Gibson, J., and Lawler, J.J. 2007. "Random forests for classification in ecology." *Ecology*, Vol. 88(No. 11): pp. 2783–2792. doi:10.1890/07-0539.1.

Eskelson, B.N.I., Barrett, T.M., Temesgen, H. 2009. "Imputing mean annual change to estimate current forest attributes." *Silva Fennica*, Vol. 43(No. 4): pp. 649–658. doi:10.14214/sf.185.

Evans, J.S, and Hudak, A.T. 2007. "A multiscale curvature algorithm for classifying discrete return LiDAR in forested environments." *IEEE Transactions on Geoscience and Remote Sensing*, Vol. 45(No. 4): pp. 1029–1038. doi:10.1109/TGRS.2006.890412.

Evans, J.S, and Murphy, M.A. 2017. "rfUtilities: Random forests model selection and performance evaluation." R package version 2.1-1. http://CRAN.R-project.org/package=rfUtilities

Falkowski, M.J., Evans J.S., Martinuzzi, S., Gessler, P.E., and Hudak, A.T. 2009. Characterizing forest succession with lidar data: "An evaluation for the Inland Northwest, USA." *Remote Sensing of Environment*, Vol. 113: pp. 946–956. doi:10.1016/j.rse.2009.01.003.

Falkowski, M.J., Smith, A.M.S., Gessler, P.E., Hudak, A.T., Vierling, L.A., and Evans, J.S. 2008. "The influence of conifer forest canopy cover on the accuracy of two individual tree measurement algorithms using lidar data." *Canadian Journal of Remote Sensing*, Vol. 34(Sup. 6): pp. S338–S350. doi:10.5589/m08-055.

Fassnacht, F.E., Hartig, F., Latifi, H., Berger, C., Hernández, J., Corvalán, P., and Koch, B. 2014. "Importance of sample size, data type and prediction method for remote sensing-based estimations of aboveground forest biomass." *Remote Sensing of Environment*, Vol. 154: pp. 102–114. doi:10.1016/j.rse.2014.07.028.

Fekety, P.A., Falkowski, M.J., Hudak, A.T. 2015. "Temporal transferability of LiDAR-based imputation of forest inventory attributes." *Canadian Journal of Forest Research*, Vol. 45: pp. 422–435. doi:10.1139/cjfr-2014-0405.

Freeman, J.A., Moisen, G.G., Coulston, J.W., and Wilson, B.T. 2014. "Random forests and stochastic gradient boosting for predicting tree canopy cover: comparing tuning processes and model performance." *Canadian Journal of Forest Research*, Vol. 46: pp. 323–339. doi:10.1139/cjfr-2014-0562.

Gleason C.J. and Im, J. 2012. "Forest biomass estimation from airborne LiDAR data using machine learning approaches." *Remote Sensing of Environment*, Vol. 125: pp. 80–91. doi:10.1016/j.rse.2012.07.006

Goodwin, N.R., Coops, N.C., Culvenor, D. S. 2006. "Assessment of forest structure with airborne LiDAR and the effects of platform altitude." *Remote Sensing of Environment*, Vol. 103: pp. 140–152. doi:10.1016/j.rse.2006.03.003.

GRASS Development Team. 2017. Geographic Resources Analysis Support System (GRASS) Software, Version 7.2. Open Source Geospatial Foundation. http://grass.osgeo.org

Hayashi R., Kershaw, J.A. Jr., Weiskittel, A. 2015. "Evaluation of alternative methods for using LiDAR to predict aboveground biomass in mixed species and structurally complex forests in northeastern North America." *Mathematical and Computational Forestry & Natural Resources Sciences*, Vol. 7(No. 2): pp. 49–65.

Heidemann, H.K. 2014. "Lidar base specification (ver. 1.2, November 2014)." In *U.S. Geological Survey Techniques and Methods, book 11, chap. B4, 67 p. with appendixes.* http://dx.doi.org/10.3133/tm11B4.

Hopkinson C. 2007. "The influence of flying altitude, beam divergence, and pulse repetition frequency on laser pulse return intensity and canopy frequency distribution." *Canadian Journal of Remote Sensing*, Vol. 33(No. 4): pp. 312–324. doi:10.5589/m07-029.

Hudak, A.T., Crookston, N.L., Evans, J.S., Falkowski, M.J., Smith, A.M.S., Gessler, P.E., and Morgan, P. 2006. "Regression modeling and mapping of coniferous forest basal area and tree density from discrete-return lidar and multispectral satellite data." *Canadian Journal of Remote Sensing*, Vol. 32: pp. 126–138.

Hudak, A.T., Strand, E.K., Vierling, L.A., Byrne, J.C., Eitel, J.U.H., Martinuzzi, S., and Falkowski, M.J. 2012. "Quantifying aboveground forest carbon pools and fluxes

from repeat LiDAR surveys." *Remote Sensing of Environment* 123: pp. 25–40. doi:10.1016/j.rse.2012.02.023.

Kimsey, M.J. Jr., Moore, J., and McDaniel, P. 2008. "A geographically weighted regression analysis of Douglas-Fir Site Index in North Central Idaho." *Forest Science*, Vol. 54(No. 3): pp. 356–366.

Latifi, H. and Koch, B. 2012. "Evaluation of most similar neighbour and random forest methods for imputing forest inventory variables using data from target and auxiliary stands." *International Journal of Remote Sensing*, Vol. 33(No. 21): pp. 6668–6694. doi:10.1080/01431161.2012.693969.

Lawrence, R.L., Wood, S.D., and Sheley, R.L. 2006. "Mapping invasive plants using hyperspectral imagery and Breiman Cutler classifications (RandomForest)." *Remote Sensing of Environment*, Vol. 100: pp. 356–362. doi:10.1016/j.rse.2005.10.014.

Lefsky, M.A., Cohen, W.B., Harding, D.J., Parker, G.G, Acker, S.A., and Gower, S.T. 2002. "Lidar remote sensing of above-ground biomass in three biomes." *Global Ecology and Biogeography*, Vol. 11(No. 5): pp. 393–399. Available from http://www.treesearch.fs.fed.us/pubs/24647.

Liaw, A. and Wiener, M. 2002. "Classification and Regression by randomForest." *R News*, Vol. 2(No. 3), pp. 18–22. Available from https://cran.r-project.org/doc/Rnews/.

Maltamo, M., Næsset, E., and Vauhknen, J. (Editors) 2014. *Forestry Applications of Airborne Laser Scanning Concepts and Case Studies*. Dordrecht, Netherlands: Springer Science + Business Media.

Martinuzzi, S., Vierling, L.A., Gould, W.A., Falkowski, M.J., Evans, J.S., Hudak, A.T., and Vierling, K.T. 2009. "Mapping snags and understory shrubs for a LiDAR-based assessment of wildlife habitat suitability." *Remote Sensing of Environment*, Vol. 113: pp. 2533–2546. doi:10.1016/j.rse.2009.07.002.

McGaughey, R.J. 2016. "FUSION/LDV: Software for LIDAR data analysis and visualization, version 3.60+." USDA For. Serv., Pacific Northwest Research Station, Portland, OR. 206 pp. http://forsys.cfr.washington.edu/fusion/FUSION_manual.pdf.

MNGeo 2015. "LiDAR elevation data for Minnesota [online]." http://www.mngeo.state.mn.us/chouse/elevation/lidar.html [accessed 01 December 2015].

Murphy, M., Evans, J.S., and Storfer, A. 2010. "Quantifying Bufo boreas connectivity in Yellowstone National Park with landscape genetics." *Ecology*, Vol. 91: pp. 252–261. doi:10.1890/08-0879.1.

Næsset, E. 2002. "Predicting forest stand characteristics with airborne scanning laser using a practical two-stage procedure and field data." *Remote Sensing of Environment*, Vol. 80: pp. 88–99. doi:10.1016/S0034-4257(01)00290-5.

Næsset, E. 2004. "Practical large-scale forest stand inventory using a small-footprint laser scanner." *Scandinavian Journal of Forest Research*, Vol. 19: pp. 164–179. doi:10.1080/02827580310019257.

Næsset, E. 2007. "Airborne laser scanning as a method in operational forest inventory: Status of accuracy assessments accomplished in Scandinavia." *Scandinavian Journal of Forest Research*, Vol. 22: pp. 433–442. doi:10.1080/02827580701672147.

Næsset, E. 2009. "Effects of different sensors, flying altitudes, and pulse repetition frequencies on forest canopy metrics and biophysical stand properties derived from small-footprint airborne laser data." *Remotes Sensing of Environment*, Vol. 113: pp. 148–159. doi:10.1016/j.rse.2008.09.001.

Penner, M., Pitt, D.G., and Woods, M.E. 2013. "Parametric vs. nonparametric LiDAR models for operational forest inventory in boreal Ontario." *Canadian Journal of Remote Sensing*, Vol. 39(No. 5) pp. 426–443. doi:10.5589/m13-049.

Prasad, A.M., Iverson, L.R., and Liaw, A. 2006. "Newer classification and regression tree techniques: Bagging and random forests for ecological prediction." *Ecosystems*, Vol. 9: pp. 181–199. doi:10.1007/s10021-005-0054-1.

R Core Team. 2017. "R: A language and environment for statistical computing." R Foundation for Statistical Computing, Vienna, Austria. http://www.R-project.org/.

Robinson A.P. 2016." equivalence: Provides Tests and Graphics for Assessing Tests of equivalence." R package version 0.7.2. https://CRAN.R-project.org/package=equivalence.

Robinson, A.P. and Froese, R.E. 2004. "Model validation using equivalence tests." *Ecological Modelling*, Vol. 176: pp. 349–358. doi:10.1016/j.ecolmodel.2004.01.013.

Robinson, A.P., Duursma, R.A., and Marshall, J.D. 2005. "A regression-based equivalence test for model validation: shifting the burden of proof." *Tree Physiology*, Vol. 25(No. 7): pp. 903–913. doi:10.1093/treephys/25.7.903.

Stage, A.R. and Salas, C. 2007. "Interactions of Elevation, Aspect, and Slope in Models of Forest Species Composition and Productivity." *Forest Science*, Vol. 53(No. 4): pp. 486–492. Available at https://www.treesearch.fs.fed.us/pubs/29167.

Taylor, J.L. 2012. "Northern Rockies Ecoregion: Chapter 7." In *Status and trends of land change in the Western United States–1973 to 2000. USGS Publications Warehouse*. http://pubs.er.usgs.gov/publication/pp1794A7.

USFS (United States Forest Service). 2016. "Region One vegetation classification, mapping, inventory and analysis report: Common stand exam protocols for vegetation data sampling in conjunction with Lidar." Report 14-17 v2.2. Missoula, MT, USA.

Wellek, S. 2003. *Testing Statistical Hypotheses of Equivalence*. Boca Raton, FL, USA: Chapman and Hall/CRC.

White, J.C., Wulder, M.A., and Buckmaster, G. 2014. Validating estimates of merchantable volume from airborne laser scanning (ALS) data using weight scale data. *The Forestry Chronicle*, Vol 90 (No. 3) pp. 378–385.

White, J.C., Wulder, M.A., Varhola, A., Vastaranta, M., Coops, N.C., Cook, B.D., Pitt, D., and Woods, M. 2013. "A best practices guide for generating forest inventory attributes from airborne laser scanning data using an area-based approach." Canadian Forest Service Canadian Wood Fibre Centre Information Report FI-X-010. http://cfs.nrcan.gc.ca/pubwarehouse/pdfs/34887.pdf.

Zald, H.S.J., Ohmann, J.L., Roberts, H.M., Gregory, M.J., Henderson, E.B., McGaughey, R.J., and Braaten, J. 2014. "Influence of lidar, Landsat imagery, disturbance history, plot location accuracy, and plot size on accuracy of imputation maps of forest composition and structure." *Remote Sensing of Environment*, Vol. 143: pp. 26–38. doi:10.1016/j.rse.2013.12.013.